

First Experiments with the ITER-Relevant LHCD Launcher in Tore Supra

A. Ekedahl, L. Delpech, M. Goniche, D. Guilhem, J. Hillairet, M. Preynas, P.K. Sharma¹, J. Achard, Y.S. Bae², X. Bai³, C. Balorin, Y. Baranov⁴, V. Basiuk, A. Bécoulet, J. Belo⁵, G. Berger-By, S. Brémond, C. Castaldo⁶, S. Ceccuzzi⁶, R. Cesario⁶, E. Corbel, X. Courtois, J. Decker, E. Delmas⁷, X. Ding³, D. Douai, C. Goletto, J.P. Gunn, P. Hertout, G.T. Hoang, F. Imbeaux, J. Kim², K.K. Kirov⁴, S. Lee², X. Litaudon, R. Magne, J. Mailloux⁴, D. Mazon, F. Mirizzi⁶, P. Mollard, P. Moreau, T. Oosako, V. Petrzelka⁸, Y. Peysson, S. Poli, M. Prou, F. Saint-Laurent, F. Samaille, B. Saoutic

CEA, IRFM, 13108 Saint Paul-lez-Durance, France.

¹ Permanent address: Institute for Plasma Research, Bhat, Gandhinagar, Gujarat, India.

² National Fusion Research Institute, Daejeon, South Korea.

³ Southwestern Institute of Physics, Chengdu, P.R. China.

⁴ Euratom/CCFE Fusion Association, Culham Science Centre, Abingdon, OX14 3DB, UK.

⁵ Associação Euratom-IST, Centro de Fusão Nuclear 1049-001 Lisboa, Portugal.

⁶ Associazione Euratom-ENEA sulla Fusione, CR Frascati, Roma, Italy.

⁷ Present address: ITER Organization, 13067 Saint Paul-lez-Durance, France.

⁸ Association Euratom-IPP.CR, Za Slovankou 3, 182 21 Praha 8, Czech Republic.

Introduction. This paper presents the first experimental results obtained with the ITER-relevant lower hybrid current drive (LHCD) launcher in Tore Supra. The launcher is based on the passive active multijunction (PAM) concept [1-3], which is the design proposed for an ITER LHCD system [4, 5]. The PAM design allows efficient cooling of the waveguides, in order to sustain the heat load during long pulses. In addition, it offers low power reflection close to the cut-off density ($n_{co} = 1.7 \times 10^{17} \text{ m}^{-3}$ at $f = 3.7 \text{ GHz}$), which is important in view of ITER, where the large distance between the plasma and the wall may bring the density in front of the launcher to low values. The main goals of the first experimental campaign with the PAM in Tore Supra were to: i) compare the power reflection coefficient (RC) on the PAM to the predictions from the ALOHA code [6], ii) demonstrate reliable power coupling during edge perturbations mimicking ELMs and iii) achieve ITER-relevant power density, i.e. 25 MW/m^2 at $f = 3.7 \text{ GHz}$ [5], in pulse lengths of several tens of seconds. These goals were achieved. In addition, full non-inductive discharges lasting 50s were performed.

Coupling characteristics. The power reflection coefficient (RC) on the PAM launcher has been studied in dedicated coupling experiments carried out at low power (200 kW , $\sim 2 \text{ MW/m}^2$) in order to avoid possible non-linear effects that can occur at high power [7]. The density at the launcher mouth was varied from $0.5 \times 10^{17} \text{ m}^{-3}$ to $8 \times 10^{17} \text{ m}^{-3}$ by varying the plasma-launcher distance during the pulse. Fig. 1 shows the measured RC, averaged over the 16 modules, versus the electron density at the launcher mouth, as measured by Langmuir probes on the launcher. 180° phasing between active waveguides was used, giving peak parallel refractive

index $n_{\parallel} = 1.72$. Good coupling, i.e. $RC < 2\%$, is obtained in the vicinity of the cut-off density. The solid curves correspond to the ALOHA code predictions, using different density decay lengths in the scrape-off layer (SOL). Two density layers are usually required to describe the experimental results satisfactorily. The first layer ($\lambda_{n1} \sim \text{mm}$) describes the private SOL between the side protections on the launcher, while the second layer ($\lambda_{n2} \sim \text{cm}$) describes the main SOL. Good agreement between experiment and modelling is obtained.

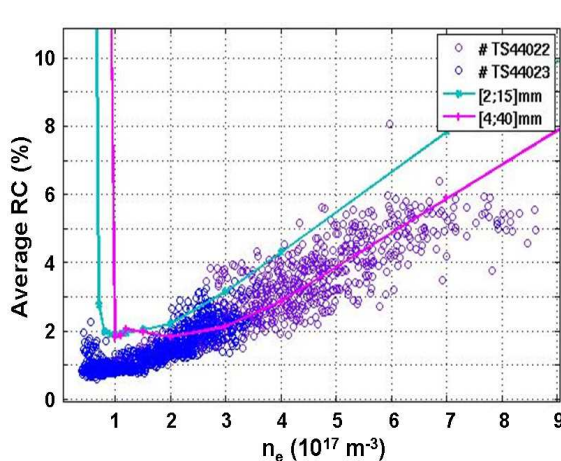


Fig. 1: Reflection coefficient on the PAM launcher versus electron density at the launcher mouth. Good agreement with the ALOHA code results is obtained.

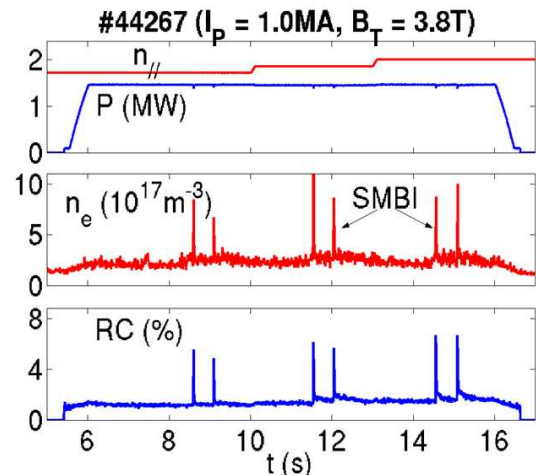


Fig. 2: RC behaviour during edge perturbations produced by SMBI. RC increases in accordance with the coupling code prediction.

Coupling with edge perturbations. LHCD experiments were also carried out in the presence of edge perturbations, produced by supersonic molecular beam injection (SMBI) to simulate ELM-behaviour. During a SMBI, the electron density in front of the launcher increases from $\sim 2 \times 10^{17} \text{ m}^{-3}$ to $\sim 10 \times 10^{17} \text{ m}^{-3}$ and the RC increases from 1.5% to 7% (Fig. 2), in accordance with the coupling code prediction. At least at intermediate power level (1.5MW, 13MW/m²), the applied power remained constant during SMBI, indicating the possibility to couple during edge perturbations, such as ELMs. Note that the present ITER PAM design [8] will give smaller variation in RC during an increase in density, making it a more ELM-resilient system. In these experiments, the evolution of the hard X-ray emission (< 200keV) from the suprathermal electrons was studied during SMBI, as well as versus LHCD power, n_{\parallel} and electron density. During each SMBI, the hard X-ray signal falls, but the slow response of the hard X-ray emission suggests that it is due to the perturbation of the bulk density. The hard X-ray emission profile remains the same before and during SMBI, which indicates that the edge perturbation itself does not cause a redistribution of the fast electron profile [9].

High power operation. The maximum power and energy achieved on the PAM launcher so far is 2.75MW during 78s (Fig. 3), obtained after ~ 400 pulses on plasma. This corresponds to

a power density of 25MW/m^2 , which is equivalent to the design value for an ITER LHCD system (33MW/m^2 at $f = 5\text{GHz}$) [5]. At the present stage, the limitation is partly due to lack of generator power, partly due to conditioning. In addition, 2.75MW was coupled at a plasma-launcher distance of 10cm, with RC as low as 2% (Fig. 3). The density in front of the launcher was still above the cut-off density in these conditions, since the plasma scenario used was characterized by long SOL density decay length ($\lambda_n \sim 4\text{cm}$). The launcher front face protection, based on the CuXIX-line emission and infrared thermography, detected very few arcs at the launcher mouth during the experiments. The temperature of the waveguides and the side protections, which are actively cooled, remained below 300°C (Fig. 4).

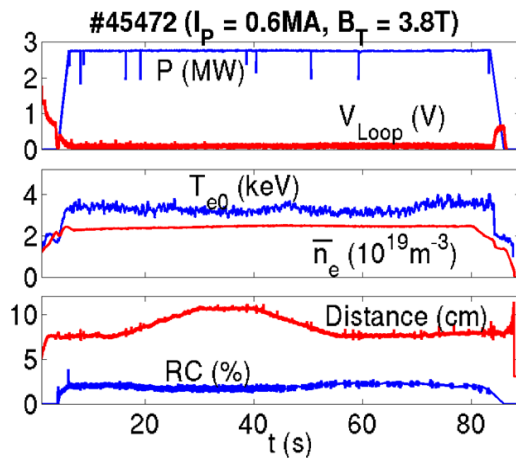


Fig. 3: Maximum power and energy achieved on the PAM launcher (2.75MW, 78s). The plasma-launcher distance is ramped to 10cm.

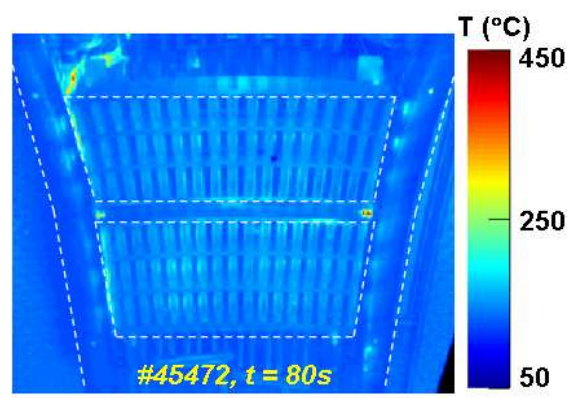


Fig. 4: Infrared image of the PAM launcher during pulse #45472. The waveguides and side protections, actively cooled, remain below 300°C .

The intensity of the fast electron beam in front of the waveguide rows (caused by parasitic absorption at the launcher mouth and responsible for hot spots on plasma facing components) was investigated by detailed radial-poloidal mappings using a retarding field analyser, as described in [10]. The first results indicate that the parasitic electron beam is less intense with the PAM launcher, compared to what was previously observed with a full active multijunction (FAM) launcher under similar experimental conditions [10]. This result remains however to be confirmed in experiments with PAM and FAM on the same plasma target.

Non-inductive current drive. Full non-inductive pulses lasting up to 50s have been performed with the PAM launcher, using real-time control loops to maintain the plasma current constant by adjusting the LH power and to maintain the primary flux consumption at zero by acting on the central solenoid voltage. $P_{\text{LH}} = 2.2\text{MW}$ was required to maintain $I_P = 0.5\text{MA}$ and $V_{\text{Loop}} = 0$ at $\bar{n}_e = 1.45 \times 10^{19}\text{m}^{-3}$. Parallel refractive index $n_{\parallel} = 1.72$ was used, which corresponds to the optimum value, i.e. giving highest power directivity on the PAM.

The current drive efficiency is approximately $0.8 \times 10^{19} \text{ m}^{-2} \text{ A/W}$, which is $\sim 10\%$ higher than in the GJ-discharges in Tore Supra, carried out with the two FAM launchers, using $n_{\parallel} = 1.72$ [11]. It should be noted that the power directivity was not maximized in the GJ-discharges, since the FAM launchers have maximum power directivity at $n_{\parallel} = 1.83$ and 2.03, respectively. Further experiments will allow comparing the CD efficiency for PAM and FAM.

Finally, experiments have also been conducted with the aim to study the CD efficiency at high electron density (up to $\bar{n}_e = 6 \times 10^{19} \text{ m}^{-3}$). Although full non-inductive current drive could not be obtained at such high densities, the evolution of the hard X-ray emission was studied [12].

Summary and outlook. The first experiments with the ITER-relevant LHCD PAM launcher in Tore Supra have shown extremely encouraging results in terms of coupling behaviour and power handling. Good agreement between the experimental reflection coefficient and the ALOHA code prediction is obtained. The design value for the power density (i.e. 25 MW/m^2) has been obtained over pulse lengths up to 78s. High power (2.75MW) has been coupled at a plasma-launcher distance of 10cm with a power reflection coefficient as low as 2%. These results give confidence that the PAM concept is a viable design for an ITER LHCD system. The completion of the Tore Supra CIMES project, consisting of an upgrade of the LH transmitter plant with 700kW/CW klystrons [13], will allow to increase the available LHCD power and to access regimes of zero loop voltage at higher current and density than before.

Acknowledgements. The authors gratefully acknowledge the support of the Tore Supra Team, in particular of the CIMES project team. This work, supported by the European Communities under the contract of Association between EURATOM and CEA, was carried out within the framework of the European Fusion Development Agreement. The views and opinions expressed herein do not necessarily reflect those of the European Commission.

References:

- [1] J. Belo, Ph. Bibet et al., *Fusion Eng. Des.* **74** (2005) 283.
- [2] V. Pericoli Ridolfini et al., *Nucl. Fusion* **45** (2005) 1085.
- [3] D. Guilhem et al., Proc. 18th Topical Conf. on RF Power in Plasmas, Gent. AIP Conf. Proc. **1187** (2009) 435.
- [4] Ph. Bibet et al., *Fusion Eng. Des.* **74** (2005) 419.
- [5] G.T. Hoang et al., *Nucl. Fusion* **49** (2009) 075001.
- [6] J. Hillairet et al., *Fusion Eng. Des.* **84** (2009) 953.
- [7] A. Ekedahl et al., Proc. 18th Topical Conf. on RF Power in Plasmas, Gent. AIP Conf. Proc. **1187** (2009) 407.
- [8] J. Hillairet et al., To be presented at 26th SOFT, Porto (2010).
- [9] P.K. Sharma et al., This conference, Paper P5.184.
- [10] J.P. Gunn et al., *Journal Nuc. Mat.* **390-391** (2009) 904.
- [11] D. VanHoutte et al., *Nucl. Fusion* **44** (2004) L11.
- [12] M. Goniche et al., This conference, Paper I2.107.
- [13] F. Kazarian et al., *Fusion Eng. Des.* **84** (2009) 1006.